Structure-Preserving Extremely Low Light Image Enhancement with Fractional Order Differential Mask Guidance

Yijun Liu
University of Electronic Science and Technology of China
liuyijungoon@163.com

Zhengning Wang*
University of Electronic Science and Technology of China
zhengning.wang@uestc.edu.cn

Ruixu Geng
University of Electronic Science and Technology of China
ruixugeng@gmail.com

Hao Zeng
University of Electronic Science and Technology of China
haozeng@std.uestc.edu.cn

Yi Zeng
University of Electronic Science and Technology of China
2567095524@qq.com

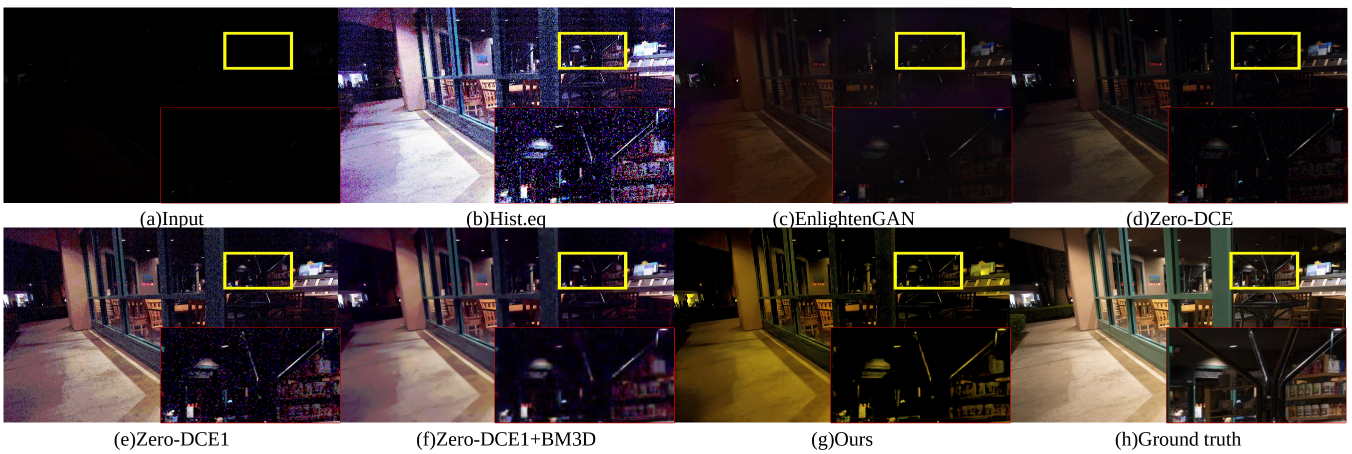

Figure 1: Given a low-light sRGB image of 24-bit color depth (a), typical enhancement methods cannot produce a pleasant image with details recovered and noise suppressed (b)-(f). (e) is Zero-DCE net retrained with original data and low-light sRGB images. (f) is the image obtained after further denoising operation with BM3D algorithm based on (e).

ABSTRACT

Low visibility and high-level noise are two challenges for low-light image enhancement. In this paper, by introducing fractional order differential, we propose an end-to-end conditional generative adversarial network(GAN) to solve those two problems. For the problem of low visibility, we set up a global discriminator to improve the overall reconstruction quality and restore brightness information. For the high-level noise problem, we introduce fractional order differentiation into both the generator and the discriminator. Compared with conventional end-to-end methods, fractional order can better distinguish noise and high-frequency details, thereby achieving superior noise reduction effects while maintaining details. Finally, experimental results show that the proposed model obtains superior visual effects in low-light image enhancement. By introducing fractional order differential, we anticipate that our framework will enable high quality and detailed image recovery not only in the field of low-light enhancement but also in other fields that require details.

MMAsia '20, March 7–9, 2021, Virtual Event, Singapore

ACM ISBN 978-1-4503-8308-0/21/03…$15.00
https://doi.org/10.1145/3444685.3446319

KEYWORDS

image enhancement, fractional order differential, GAN

1 INTRODUCTION

Low-light image enhancement research has gained growing popularity in recent years. The visibility of low-light images in the standard RGB space does not match with human perception, due to quantization. For images taken in an extremely dark environment, they suffer from low SNR, loss of texture detail, and color degraded. Low-light image enhancement has a wide range of applications and significant impact on the performance of various tasks, such as target tracking, object detection, medical image analysis and so on. Hence, enhancing low-light image and recovering the hidden details are very important for many image processing applications.

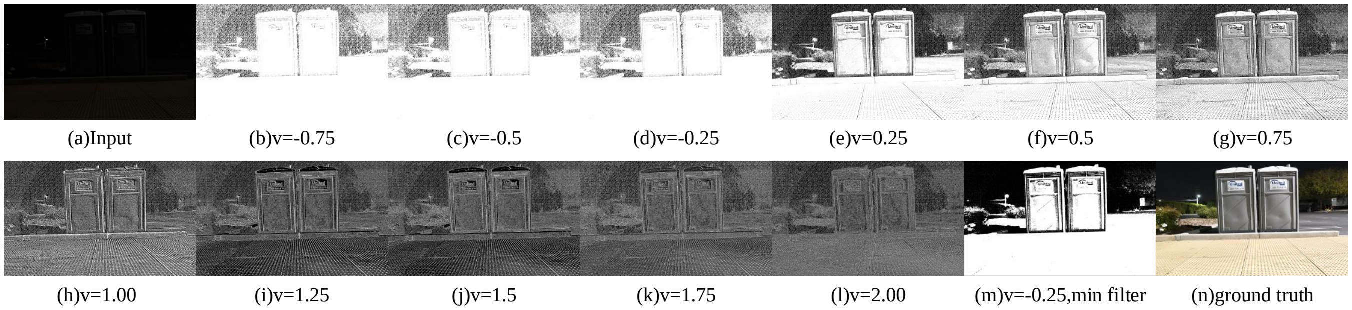

Figure 2: (b)-(l) are the fractional order gradient masks obtained when the fractional order v ranges from -0.75 to 2, and the interval is 0.25. (m) is the fractional order gradient masks obtained by Minimum filtering operation on (e).

However, most of the existing advanced methods[10, 11, 14, 29] for image enhancement rely on lower noise images as input. There is basically no loss of texture details and no noise interference. So, they cannot be used to enhance the majority of the practical low-light images with noise. Existing enhancement methods may either enhance both the noise and scene details which are not match with human perception[11, 29], or fail to recover the visibility of low-light images[10, 14].

In this paper, we proposed an image enhancement method and test on standard RGB (sRGB, 24bits/pixel) images while solving denoising problems. Our work is inspired by various gradient-guided tasks, considering the fractional order differential operation[6, 25] is much better for preserving the visual appearance as compared to traditional integer-order methods. Partially, we bring the fractional order differential theory to the low-light image enhancement.

We observe that fractional order differential operators with different orders have different detection capabilities for detail texture and noise, as shown in Fig. 2. From (m) in Fig. 2, it can be found that negative order differential ($v < 0$) has a strong ability to detect texture details, by which the flat surface of the image appears large white area. On the other hand, performing minimum filtering on the obtained fractional order mask can suppress noise (as shown in the sky in Fig. 2(m).) and increase the contrast of important textures. For exchange, parts of the fine texture are lost as the cost of suppressing noise. In addition, we choose $v = 0.75$ as the fractional order gradient detection on the restored image to provide a trade off between suppressing noise and increasing textures.

Generative adversarial networks (GANs), famous for their ability to generate visual realistic images, are adopted in our framework. Inspired by [33], the generator part is based on U-Net and fractional order branch is added to get detailed features. Two discriminators are used to discriminate the restored image and the fractional order differential mask the restored image respectively.

To summarize, our main contributions are:

(1) We introduce fractional order differential operation into image enhancement. Experimental results proved that the model with fractional order differential can better capture detailed information and restore more realistic images.
(2) We propose a creative generator structure, which combines global information and detailed information, implemented on the basis of U-Net. By extending downsampling to two branches, our proposed generator can take into account both global information and detailed texture to obtain more realistic reconstruction results.
(3) We present a framework including one generator and two discriminators using order differential differentiation which obtain state-of-the art NIQE results in low-light image enhancement.

2 RELATED WORKS

2.1 Low-light image enhancement.

A kind of low-light image enhancement methods[2, 7, 11, 28] is based on the Retinex theory. They decompose the input low-light image into illumination and reflectance and enhance the illumination of the image and suppress noise. Another kind of methods adopts advanced learning-based technique to enhance high-quality user retouched images or images taken using high-end cameras, such as using bilateral learning [8], intermediate HDR supervision [32], adversarial learning [4, 12, 14], and reinforcement learning [21].

There are few researches focusing on extremely dark image enhancement. The state-of-the-art work, Zero-Reference Deep Curve Estimation(Zero-DCE net)[10] , formulates low light image enhancement as a task of image-curve estimation with four losses. Like the curves adjustment used in photo editing software, Zero-DCE net enhances both the image objectives and noise. If the parameters trained through the dataset given in the paper are used to enhance our data, there is a problem of insufficient illumination enhancement. After adding our dark image data to the original data and retraining the network, the test images have some color distortion and noise enhancement. Advanced work EnlightenGAN[14] found that the Vgg-based perceptual loss[15] of low-light images and normal images is similar. Hence, the paper utilize this principle to maintain the correlation between input and output, which results in EnlightenGAN not changing the texture of the image and suppressing noise. Therefore, EnlightenGAN is not suitable for image enhancement that handles extremely low illumination.

Chen et al. [3] present models learned from raw images. However, models trained on the raw domain can not be applied to regular sRGB images, which is the most widely adopted color space, as the linear raw data is significantly different from the non-linear sRGB data [31]. Besides, raw data is usually unavailable due to a lack of expertise or unknown protocols. Xu et al.[30] propose a frequency-based decomposition and enhancement model to solve the problems. We tried to deal with the same problem as the above paper. Instead of decomposing the frequency, we used the method of fractional order gradient mask guidance. The images we recovered are not as bright as they recovered, but they are in line with human visual perception.

2.2 Fractional order differential operator

As a conventional theory, fractional order derivative provides the flexibility of enhancing the complex textural details of an image in a nonlinear manner[23]. It can maintain the low-frequency contour features in the smooth area of an image in a nonlinear fashion and creates the possibility of enhancing the high-frequency edges and textural details in a nonlinear manner. At the same time, fractional order differential is extremely sensitive to the small change of pixel value, so it can detect the noise effectively.

3 APPROACH

3.1 Overview and Motivation

Extremely low illumination image enhancement is a comprehensive task involving color restoration, noise suppression, and texture restoration. One of the biggest problems with very low illuminance image enhancement is that there are areas without any useful information in numerous images, but there is a lot of noise in this area, and ground truth has a clear target at the corresponding position, as shown in Fig. 3. As a result, if we do not impose constraints, the network would infer some strange targets based on the distribution of noise. It is quite difficult to recover the texture details from a large amount of noise, so we choose to suppress this part of the noise and keep the image partially dark.

Zero-DCE net is an excellent job by adjusting pixels through curves. However, there is a problem of insufficient brightness enhancement. The enhanced image is fairly natural and slightly brightened. Therefore, we choose the Zero-DCE net enhanced image as the input of further enhancing image to reduce the difficulty of the enhancement of deep dark images.

Our method is also inspired by various gradient-guided tasks [18, 34] for super-resolution and or inpainting. Compared with traditional differential operators, fractional order differential operators have better performance in detecting and saving textures. When the order v of the fractional order differential mask takes different values, it has different performances for texture detection, as shown in Fig. 2. When v takes a negative value(take $v = -0.25$ as an example), a large area of white will appear where there is a lot of texture. In dark areas, such as the sky, the textures are all derived from noise and will be relatively small. The background color of the area is large black. Then, we perform minimum filtering on it, which greatly reduces the noise in dark areas, such as the sky. We input the obtained mask into the network to guide the network to suppress noise.

In addition, we found that when v is equal to 0.75, the input dark image and ground truth bright image have better texture detection performance. Therefore, we use a fractional order differential mask with v equal to 0.75 to judge the similarity between the restored image and the ground truth. We observe images of 3 channels in RGB color space have quite different fractional order differential gradient information, as shown in Fig. 3. So we choose to calculate the fractional order differential gradient mask of the three channels separately when calculating loss and in the discriminator.

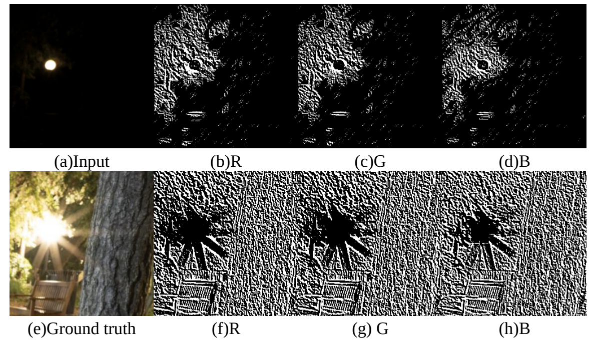

Figure 3: (b)-(d) and (f)-(h) are the fractional order differential masks of the R, G, and B channels of the input image and the ground truth image respectively.

Our framework is based on Generative Adversarial Network, as shown in Fig. 4(a). Although Zero-DCE net has the problem of insufficient illumination enhancement for extremely low-illuminance images, it runs fast and does not cause image distortion. Therefore, we use it to preprocess the input image to reduce the difficulty of network enhancement. In addition, the framework has two patchGAN[13, 17] discriminators, which distinguish the image and the fractional order differential mask of the image. The loss of the generator consists of 4 parts, namely WGAN loss, perceptual loss, L1 loss and L1 loss of fractional order differential masks.

3.2 Architecture

Fractional Order Differential Gradient Mask . The commonly used fractional order calculus definitions are those of Grünwald Letnikov, Riemann Liouville, and Caputo [20, 27]. The Grünwald-Letnikov definition of fractional order calculus, in a convenient form, for causal signal $f(x)$ is defined by:

$$D_x^v f(x) = \lim_{N\to\infty} \left\{ \frac{\left(\frac{x-a}{N}\right)^{-v}}{\Gamma(-v)} \sum_{k=0}^{N-1} \frac{\Gamma(k-v)}{\Gamma(k+1)} f\left(x - k\left(\frac{x-a}{N}\right)\right) \right\} \quad (1)$$

where $f(x)$ is a differintegrable function, $[a, x]$ is the duration of $f(x)$, v is a non-integer, $\Gamma(\alpha) = \int_0^\infty e^{-x} x^{\alpha-1} dx = (\alpha-1)!$ is the Gamma function, and D_x^v denotes the v-order fractional order differential operator.

In the work[24], Pu et al. proposed six fractional order differential operators and discuss the capability of fractional order differential masks for texture enhancement. The process of obtaining the mask is a very complicated mathematical derivation process, here we just use fractional order differential operator in one direction to get fractional differential masks, as shown in Fig. 4(b).

The fractional order differential mask of a picture can be obtained by convolution on the input image and the fractional order differential operator.

$$M_{frac} = I_R * F_{frac} \quad (2)$$

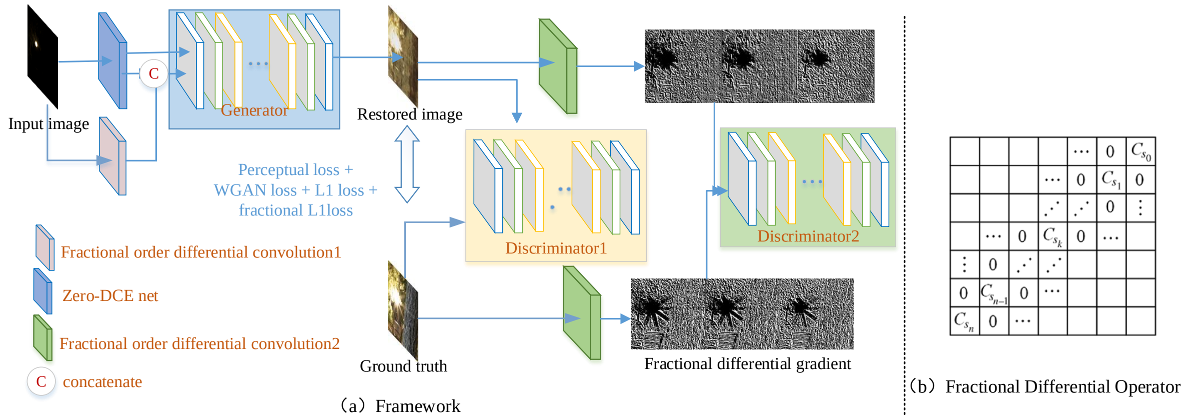

Figure 4: (a) is the overall architecture of our framework. There is 1 generator and 2 discriminators identify the image and the fractional order differential gradient mask of the image respectively. The order v of fractional order differential convolution 1 is -0.25, and the order v of fractional order differential convolution 2 is 0.75. (b) is fractional order differential operator.

where M_{frac} is the fractional order differential gradient mask, I_R is a 2-dimensional R channel image of the input image, F_{frac} is fractional order differential operator, $*$ represents convolution operation. The specific value of F_{frac} is obtained by formula 3.

$$\begin{cases} C_{s_0} = 1 \\ C_{s_1} = -v \\ \cdots \\ C_{s_{n-1}} = \frac{\Gamma(n-v-1)}{(n-1)!\Gamma(-v)} \\ C_{s_n} = \frac{\Gamma(n-v)}{n!\Gamma(-v)} \end{cases} \tag{3}$$

Generator. The network architecture of the generator is shown in Fig. 5. The generator takes a low light image as input and reconstructs a brightened image. The input and output sizes are expected to be 512×512 to extract enough features. Inspired by U-net [26], it has two downsampling branches representing the overall features and fractional order features of input images respectively, which are concatenated together to upsampling in one branch. One of the core elements of the proposed generator is the fractional order differential mask, which is calculated as the following steps. First, given that the R channel image has the richest details, the R channel image of the input RGB image is extracted to convolve with the fractional order differential operator. Then, perform minimum filtering on the obtained fractional order gradient map to get the fractional order mask of the image.

As illustrated in Fig. 5, the first downsampling branch directly performs convolution operators on the input to extract features, identical with U-Net. Simultaneously, the other downsampling branch concatenates the obtained fractional order differential mask with the input image to get a feature map with 4 channels, and then downsampling with same operators. When the first branch is down-sampled to 64x64, we perform dilation convolution to expand the receptive field of the image, after which concatenating the 64x64 feature maps of the two branches together to expand the channel of the feature maps. Finally, like U-net, we expand the size of the feature map through bilinear interpolation upsampling branch by concatenating the corresponding feature maps of the second branch together and convolution.

It can be seen that in the proposed generator, fractional order differential mask and U-Net are cleverly combined exploiting two branches. In fact, the two downsampling branches represent the global information and fractional order differential information of the input image respectively. Through such a generator structure, we can obtain reconstruction results that take into account both overall features and detailed information.

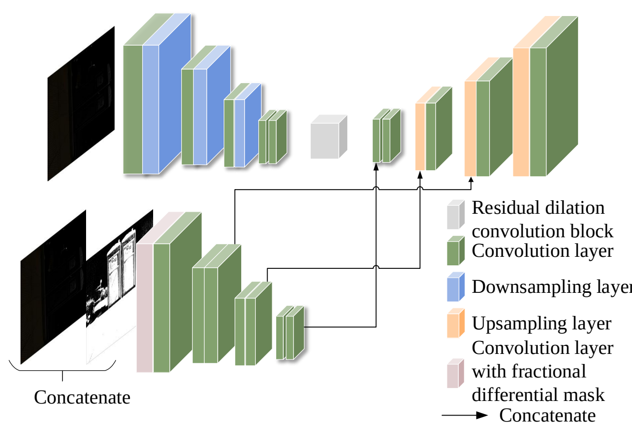

Figure 5: Generator architecture. It consists of two downsampling branches and one upsampling branch.

Discriminator. Two discriminators D_1, D_2 are applied in the proposed network, as illustrated in Fig. 4(a). D_1 is a global discriminator that determines whether the overall information of the generated image is similar to ground truth. D_2 is a novel fractional order discriminator, which is responsible for judging whether the features of the generated image at a specific fractional order level are true.

Both D_1 and D_2 use the same structure as PathchGAN[13], and alternate training with Generator to achieve more realistic effects through game operations. Due to the difference in sample distribution, InstanceNorm is utilized as the Norm layer. After experimental verification, the global discriminator D_1 can not only make the overall characteristics of the image more realistic, but also speed up the color restoration during the training process. On the other hand, the fractional order discriminator D_2 can improve the speed of convergence in detail recovery.

3.3 Loss Function

Loss of discriminator. The discriminator and generator are alternatively trained with the discriminator loss function L_D and the generator loss function L_G. L_D uses the loss function of WGAN-GP[1, 9], as formulated in Eq. 4.

$$\begin{aligned} L_d = & \mathbb{E}_{\tilde{\mathbf{x}}\in\mathbb{P}_g}[D_1(\tilde{\mathbf{x}})] - \mathbb{E}_{\mathbf{x}\in\mathbb{P}_r}[D_1(\mathbf{x})] \\ & +\sigma_1\mathbb{E}_{\hat{\mathbf{x}}\in\mathbb{P}_{\mathbf{x}}}[\|\nabla\hat{\mathbf{x}}D_1(\hat{\mathbf{x}})\|_2 - 1]^2 \\ & +\mathbb{E}_{\tilde{\mathbf{x}}\in\mathbb{P}_g}[D_2(\tilde{\mathbf{x}})] - \mathbb{E}_{\mathbf{x}\in\mathbb{P}_r}[D_2(\mathbf{x})] \\ & +\sigma_2\mathbb{E}_{\hat{\mathbf{x}}\in\mathbb{P}_{\mathbf{x}}}[\|\nabla\hat{\mathbf{x}}D_2(\hat{\mathbf{x}})\|_2 - 1]^2 \end{aligned} \tag{4}$$

where $D(.)$ is the discriminator output and $G(.)$ is the generator output. $\mathbf{x}, \tilde{\mathbf{x}}, \hat{\mathbf{x}}$, are ground truth images, restored images, and difference between them, respectively. $\mathbb{P}_g, \mathbb{P}_r, \mathbb{P}_{\hat{\mathbf{x}}}$ are the corresponding distributions of them respectively.

Loss of generator. The generator loss function includes 4 parts, as shown in Eq. 5, they are Perceptual Loss L_p, WGAN Loss L_{gan}, element-wise loss function L_1 and fractional loss function L_{frac}.

$$L_G = L_p + \lambda_1 L_{gan} + \lambda_2 L_1 + \lambda_3 L_{frac} \tag{5}$$

Specifically, referring to the perceptual loss in DeblurGAN[16], we utilize the book of the third convolutional layer in VGG-19 as a feature map, and measuring the difference between them by MSE loss, as shown in equation 6.

$$\mathcal{L}_p = \frac{1}{W_{i,j}H_{i,j}} \sum_{m=1}^{W_{i,j}} \sum_{n=1}^{H_{i,j}} \left(\phi_{i,j}(\mathbf{x})_{m,n} - \phi_{i,j}(\tilde{\mathbf{x}})_{m,n}\right)^2 \tag{6}$$

where $\phi_{i,j}$ is the feature map obtained by the j-th convolution (after activation) before the i-th maxpooling layer within the VGG19 network, pretrained on ImageNet, $W_{i,j}$ and $H_{i,j}$ are the dimensions of the feature maps. In our work we use activations from $VGG_{3,3}$ convolutional layer. The activations of the deeper layers represents the features of a higher abstraction.

Inspired by WGAN-GP, the counter loss L_{gan} is calculated by Eq. 7. In particular, because our proposed network has two discriminators D_1 and D_2, so L_{gan} also contains two corresponding components. Compared with the content-based loss function, the anti-loss L_{gan} can make the reconstruction result more visually realistic.

$$L_{gan} = -\mathbb{E}_{\tilde{\mathbf{x}}\in\mathbb{P}_g}[D_1(\tilde{\mathbf{x}})] - \mathbb{E}_{\tilde{\mathbf{x}}\in\mathbb{P}_g}[D_2(\tilde{\mathbf{x}})] \tag{7}$$

Considering that L_p uses a high-level feature map, which can reconstruct features well but not colors well, we also use L_1 to directly measure the element-wise difference between the generated image and the target image. L_{frac} is the loss function component from the fractional order differential. By controlling the order of L_{frac}, L_{frac} can be constrained on different latent spaces to obtain different effects. In this paper, we chose the 0.75 order differential as the loss function, which complements L_p and L_1 to get better performance. Therefore, the fractional order differential loss function is shown in Eq. 8.

$$L_{frac} = \left\|\tilde{\mathbf{x}}_{frac} - \mathbf{x}_{frac}\right\|_1 \tag{8}$$

$\tilde{\mathbf{x}}_{frac}$ and $\mathbf{x}_{frac}$ are the fractional order differential gradient maps of the restored image and ground truth image.

4 EXPERIMENTS

4.1 Training Details

We prepare our training data based on the SID[3] dataset, which consists of raw data and grand truth image pairs. The low light images are taken with short exposure time and the ground truth image data are collected with long exposure time. We convert the raw data to sRGB data as the dataset of our paper.

We implemented the proposed mode in the Pytorch framework and trained it with a GTX 1080Ti GPU. During training, we randomly crop patches of resolutions 1024X1024 and then resize them to 512x512 as input. For loss minimization. We adopt the ADAM optimizer for 100 epochs with an initial learning rate of 0.0001, and the learning rate decay to zero in 100 epochs. For generator, λ_1, λ_2, λ_3 are set to 0.33, 0.001, and 0.001, respectively. During test, we resize resolution to 1056x720.

To evaluate the performance of the proposed method on enhancing low light images, we quantitatively and visually compare our method to 4 State-of-the-art enhancement methods, including Histogram equalization, EnlightenGAN, Zero-DCE net, Zero-DCE1. Zero-DCE1 is the retrained network with mixed data, consisting of original data of the zero DCE paper and low light images. We use NIQE for quantitative measurement.

4.2 Comparing to Existing Methods

Visual comparisons. We first compare the visual quality of our work with several classical or recent competing methods. The results are demonstrated in Fig. 6, where the first column shows the original low-light images, and the second to fifth columns are the images enhanced by: Histogram equalization, EnlightenGAN, Zero-DCE net, our network. In addition, the last column shows the ground truth images. We next zoom in on some details in the bounding boxes. The histogram equalization[22] method can obtain relatively good illumination enhancement, but there is a lot of noise. Zero-DCE and EnlightenGAN can obtain high-quality images for enhancing images with sufficient details. However, they have the problem of insufficient illumination enhancement when dealing with extremely low illumination images. The performance of Zero-DCE is a little better than the performance of histogram equalization, which is equivalent to adaptive histogram equalization. The image processed by Zero-DCE net may have some color distortion.

Furthermore, we added 2000 extremely low-light images to the training data of the original Zero-DCE paper, retrained Zero-DCE net and named it Zero-DCE1. Zero-DCE1 has better illumination enhancement, but it will make the noise more obvious. In order to make the picture have a better visual effect, we carry out further denoising processing on the image obtained by the Zero-DCE1

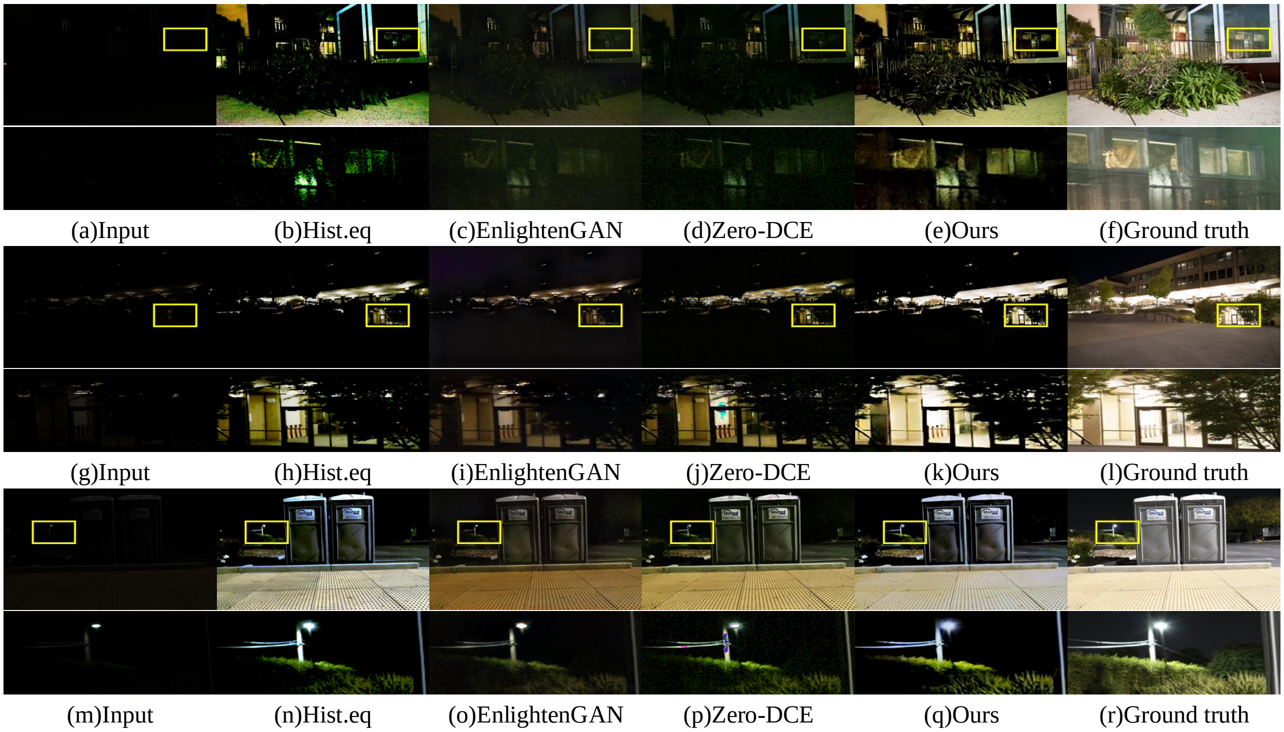

Figure 6: Visual results of state-of-the-art methods and ours on input low-light images. Yellow boxes indicate the noisy or details regions where most existing methods fail.

network using the classic denoising algorithm BM3D[5]. The result of Zero-DCE1 is shown in the figure. It can be found that Zero-DCE1 can recover the image illuminance better than Zero-DCE, but it will make the noise more obvious. This kind of noise is not easily eliminated by the BM3D algorithm.

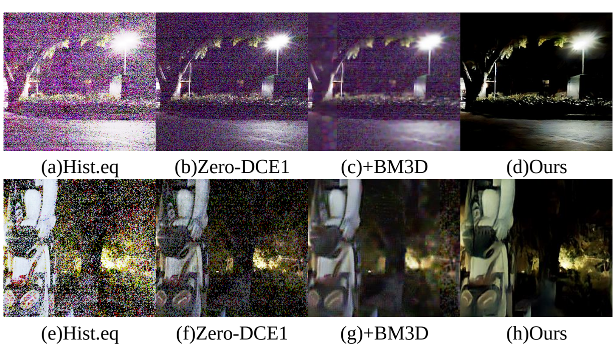

Figure 7: Zero-DCE1 retrained with our data can restore good illuminance, but make the noise more conspicuous. (c), (g) represent the results of (b), (c) denoising by BM3D algorithm. BM3D can cause blur and cannot remove noise well.

Quantitative comparisons. We adopt Natural Image Quality Evaluator (NIQE) [19], a well-known no-reference image quality assessment for evaluating image restoration to provide quantitative comparisons. The NIQE scores are reported in Table 1: a lower NIQE value indicates better visual quality.

Table 1: NIQE scores of different methods

Methods	NIQE
Hist.eq [22]	13.954
EnlightenGAN [14]	11.233
Zero-DCE [10]	12.431
Zero-DCE1 [10]	12.767
Ours	**10.659** (best)
Ground truth	8.255

5 CONCLUSIONS

In this paper, we address the low-light enhancement problem with a fractional order differential gradient mask guided framework and validate it on extremely low light dataset to show that our approach outperforms multiple state-of-the-art approaches in terms of visual quality and NIQE indicators. Improving color restoration and balancing to eliminate the problems of noise and texture detail loss are our future work. We anticipate that the generator and whole framework combining fractional order differential theory proposed here can note only provide new opportunity for dark image enhancement tasks, but also provide new tools for other tasks that require enhancement of details.

REFERENCES

[1] Martin Arjovsky, Soumith Chintala, and Léon Bottou. 2017. Wasserstein gan. *arXiv preprint arXiv:1701.07875* (2017).

[2] Bolun Cai, Xianming Xu, Kailing Guo, Kui Jia, Bin Hu, and Dacheng Tao. 2017. A joint intrinsic-extrinsic prior model for retinex. In *Proceedings of the IEEE International Conference on Computer Vision*. 4000–4009.

[3] Chen Chen, Qifeng Chen, Jia Xu, and Vladlen Koltun. 2018. Learning to see in the dark. In *Proceedings of the IEEE Conference on Computer Vision and Pattern Recognition*. 3291–3300.

[4] Yu-Sheng Chen, Yu-Ching Wang, Man-Hsin Kao, and Yung-Yu Chuang. 2018. Deep photo enhancer: Unpaired learning for image enhancement from photographs with gans. In *Proceedings of the IEEE Conference on Computer Vision and Pattern Recognition*. 6306–6314.

[5] Kostadin Dabov, Alessandro Foi, Vladimir Katkovnik, and Karen Egiazarian. 2006. Image denoising with block-matching and 3D filtering. In *Image Processing: Algorithms and Systems, Neural Networks, and Machine Learning*, Vol. 6064. International Society for Optics and Photonics, 606414.

[6] Qiang Dai, Yi-Fei Pu, Ziaur Rahman, and Muhammad Aamir. 2019. Fractional-order fusion model for low-light image enhancement. *Symmetry* 11, 4 (2019), 574.

[7] Xueyang Fu, Delu Zeng, Yue Huang, Xiao-Ping Zhang, and Xinghao Ding. 2016. A weighted variational model for simultaneous reflectance and illumination estimation. In *Proceedings of the IEEE Conference on Computer Vision and Pattern Recognition*. 2782–2790.

[8] Michaël Gharbi, Jiawen Chen, Jonathan T Barron, Samuel W Hasinoff, and Frédo Durand. 2017. Deep bilateral learning for real-time image enhancement. *ACM Transactions on Graphics (TOG)* 36, 4 (2017), 1–12.

[9] Ishaan Gulrajani, Faruk Ahmed, Martin Arjovsky, Vincent Dumoulin, and Aaron C Courville. 2017. Improved training of wasserstein gans. In *Advances in neural information processing systems*. 5767–5777.

[10] Chunle Guo, Chongyi Li, Jichang Guo, Chen Change Loy, Junhui Hou, Sam Kwong, and Runmin Cong. 2020. Zero-Reference Deep Curve Estimation for Low-Light Image Enhancement. In *Proceedings of the IEEE/CVF Conference on Computer Vision and Pattern Recognition*. 1780–1789.

[11] Xiaojie Guo, Yu Li, and Haibin Ling. 2016. LIME: Low-light image enhancement via illumination map estimation. *IEEE Transactions on image processing* 26, 2 (2016), 982–993.

[12] Andrey Ignatov, Nikolay Kobyshev, Radu Timofte, Kenneth Vanhoey, and Luc Van Gool. 2017. Dslr-quality photos on mobile devices with deep convolutional networks. In *Proceedings of the IEEE International Conference on Computer Vision*. 3277–3285.

[13] Phillip Isola, Jun-Yan Zhu, Tinghui Zhou, and Alexei A Efros. 2017. Image-to-image translation with conditional adversarial networks. In *Proceedings of the IEEE conference on computer vision and pattern recognition*. 1125–1134.

[14] Yifan Jiang, Xinyu Gong, Ding Liu, Yu Cheng, Chen Fang, Xiaohui Shen, Jianchao Yang, Pan Zhou, and Zhangyang Wang. 2019. Enlightengan: Deep light enhancement without paired supervision. *arXiv preprint arXiv:1906.06972* (2019).

[15] Justin Johnson, Alexandre Alahi, and Li Fei-Fei. 2016. Perceptual losses for real-time style transfer and super-resolution. In *European conference on computer vision*. Springer, 694–711.

[16] Orest Kupyn, Volodymyr Budzan, Mykola Mykhailych, Dmytro Mishkin, and Jiří Matas. 2018. Deblurgan: Blind motion deblurring using conditional adversarial networks. In *Proceedings of the IEEE conference on computer vision and pattern recognition*. 8183–8192.

[17] Chuan Li and Michael Wand. 2016. Precomputed real-time texture synthesis with markovian generative adversarial networks. In *European conference on computer vision*. Springer, 702–716.

[18] Cheng Ma, Yongming Rao, Yean Cheng, Ce Chen, Jiwen Lu, and Jie Zhou. 2020. Structure-Preserving Super Resolution with Gradient Guidance. In *Proceedings of the IEEE/CVF Conference on Computer Vision and Pattern Recognition*. 7769–7778.

[19] Anish Mittal, Rajiv Soundararajan, and Alan C Bovik. 2012. Making a "completely blind" image quality analyzer. *IEEE Signal processing letters* 20, 3 (2012), 209–212.

[20] Katsuyuki Nishimoto. 1996. *Fractional Calculus: Integrations and Differentiations of Arbitrary Order. Calculus in the 21st Century*. Descartes Press.

[21] Jongchan Park, Joon-Young Lee, Donggeun Yoo, and In So Kweon. 2018. Distort-and-recover: Color enhancement using deep reinforcement learning. In *Proceedings of the IEEE Conference on Computer Vision and Pattern Recognition*. 5928–5936.

[22] Stephen M Pizer, E Philip Amburn, John D Austin, Robert Cromartie, Ari Geselowitz, Trey Greer, Bart ter Haar Romeny, John B Zimmerman, and Karel Zuiderveld. 1987. Adaptive histogram equalization and its variations. *Computer vision, graphics, and image processing* 39, 3 (1987), 355–368.

[23] Yi-Fei Pu, Ni Zhang, Zheng-Ning Wang, Jian Wang, Zhang Yi, Yan Wang, and Ji-Liu Zhou. 2019. Fractional-order Retinex for adaptive contrast enhancement of under-exposed traffic images. *IEEE Intelligent Transportation Systems Magazine* (2019).

[24] Yi-Fei Pu, Ji-Liu Zhou, and Xiao Yuan. 2009. Fractional differential mask: a fractional differential-based approach for multiscale texture enhancement. *IEEE transactions on image processing* 19, 2 (2009), 491–511.

[25] Yi-Fei Pu, Ji-Liu Zhou, and Xiao Yuan. 2010. Fractional Differential Mask: A Fractional Differential-Based Approach for Multiscale Texture Enhancement. *IEEE Transactions on Image Processing* 19, 2 (Feb. 2010), 491–511. https://doi.org/10.1109/TIP.2009.2035980 Conference Name: IEEE Transactions on Image Processing.

[26] Olaf Ronneberger, Philipp Fischer, and Thomas Brox. 2015. U-net: Convolutional networks for biomedical image segmentation. In *International Conference on Medical image computing and computer-assisted intervention*. Springer, 234–241.

[27] SG Samko, AA Kilbas, and OI Marichev. 1993. Fractional Integrals and Derivatives-Theory and Applications Gordon and Breach. *Linghorne, PA* (1993).

[28] Ruixing Wang, Qing Zhang, Chi-Wing Fu, Xiaoyong Shen, Wei-Shi Zheng, and Jiaya Jia. 2019. Underexposed photo enhancement using deep illumination estimation. In *Proceedings of the IEEE Conference on Computer Vision and Pattern Recognition*. 6849–6857.

[29] Chen Wei, Wenjing Wang, Wenhan Yang, and Jiaying Liu. 2018. Deep retinex decomposition for low-light enhancement. *arXiv preprint arXiv:1808.04560* (2018).

[30] Ke Xu, Xin Yang, Baocai Yin, and Rynson WH Lau. 2020. Learning to Restore Low-Light Images via Decomposition-and-Enhancement. In *Proceedings of the IEEE/CVF Conference on Computer Vision and Pattern Recognition*. 2281–2290.

[31] Xiangyu Xu, Yongrui Ma, and Wenxiu Sun. 2019. Towards real scene super-resolution with raw images. In *Proceedings of the IEEE Conference on Computer Vision and Pattern Recognition*. 1723–1731.

[32] Xin Yang, Ke Xu, Yibing Song, Qiang Zhang, Xiaopeng Wei, and Rynson WH Lau. 2018. Image correction via deep reciprocating HDR transformation. In *Proceedings of the IEEE Conference on Computer Vision and Pattern Recognition*. 1798–1807.

[33] Zili Yi, Qiang Tang, Shekoofeh Azizi, Daesik Jang, and Zhan Xu. 2020. Contextual Residual Aggregation for Ultra High-Resolution Image Inpainting. In *Proceedings of the IEEE/CVF Conference on Computer Vision and Pattern Recognition*. 7508–7517.

[34] Jianfu Zhang, Li Niu, Dexin Yang, Liwei Kang, Yaoyi Li, Weijie Zhao, and Liqing Zhang. 2019. GAIN: Gradient Augmented Inpainting Network for Irregular Holes. In *Proceedings of the 27th ACM International Conference on Multimedia*. 1870–1878.